Supplementary Information

for Metamers of the Ventral Stream

Jeremy Freeman and Eero P. Simoncelli

Contents

Nature Neuroscience: doi:10.1038/nn.2889

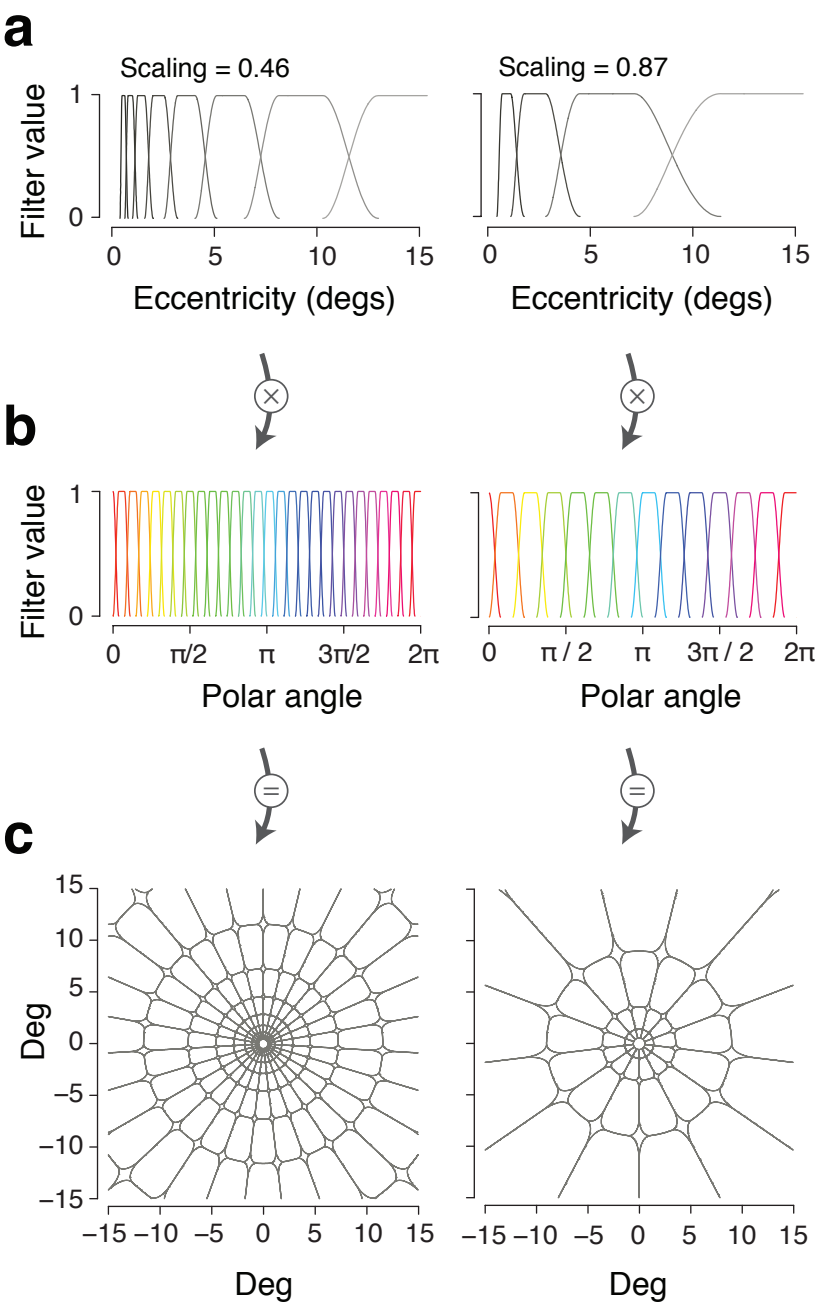

Supplementary Figure 1. Construction of spatial pooling regions using filters that are separable in log eccentricity and polar angle. **(a)** Filters have a flat top and raised cosine transition regions, and are constructed to evenly tile log eccentricity, which yields filters that grow in size with eccentricity according to a fixed scaling (ratio of size to eccentricity). Filters are shown for two scalings, 0.46 and 0.87. Filters are constructed to have approximately 50% overlap. **(b)** Similarly constructed filters are spaced evenly to tile polar angle. Larger scalings yield broader polar angle filters, to ensure that the resulting two-dimensional spatial filters have a fixed ratio of width in eccentricity to width in polar angle (see Methods). **(c)** The two separable components are combined to obtain two-dimensional spatial filters. Contours indicate the full-width half-maximum of each filter. Actual filters have soft edges and overlap by approximately 50%, as shown for the separable components in (a) and (b). The full set of filters tile evenly, and sum to a constant.

Nature Neuroscience: doi:10.1038/nn.2889

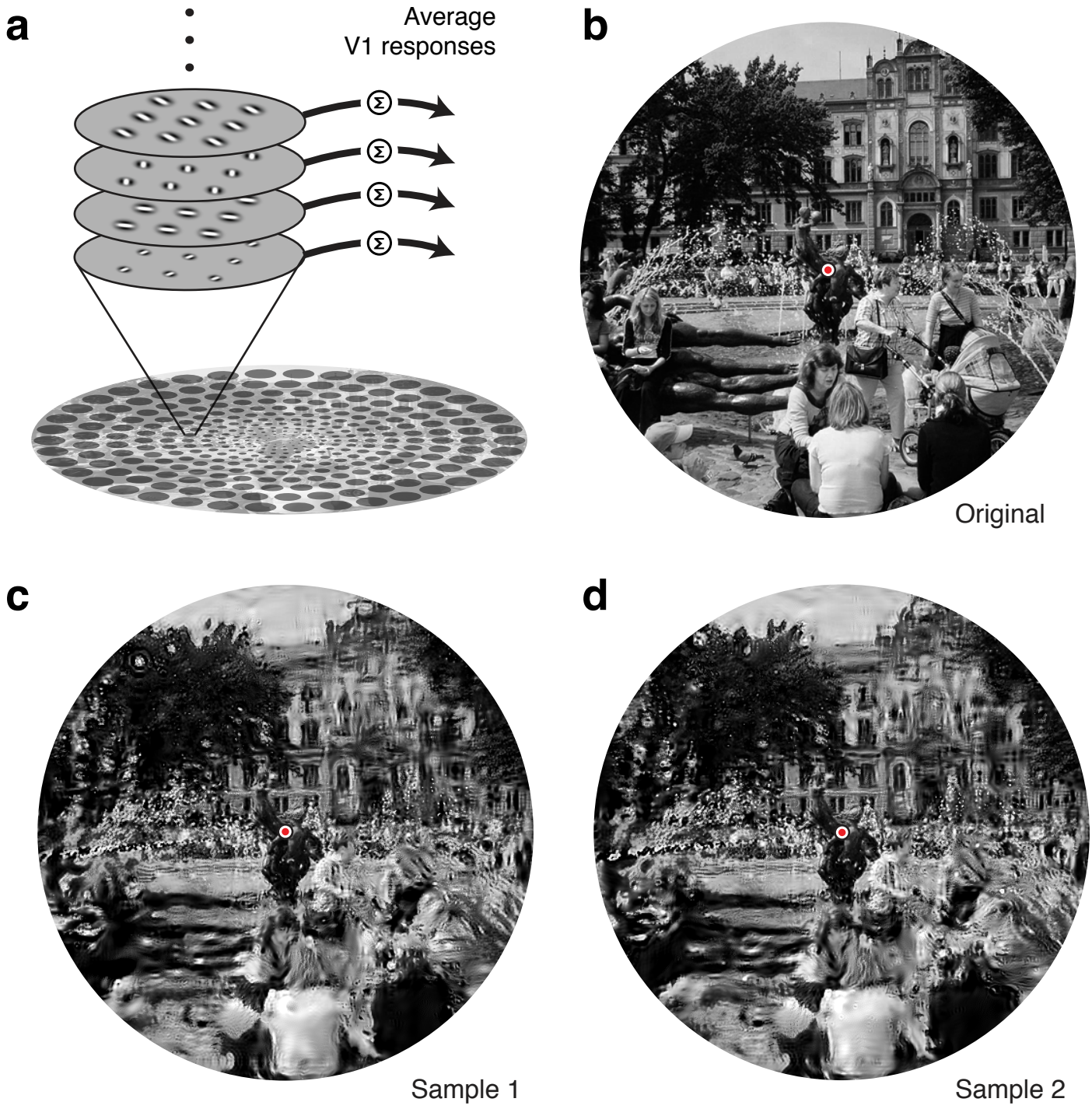

Supplementary Figure 2. V1 model and stimuli. **(a)** In each spatial pooling region, the image is represented with a bank of model V1 complex cells, varying in their preferred orientation and spatial frequency. Model responses are averages of the squared filter responses over the pooling regions. The model captures local spectral energy, but not local correlations across orientations and scales. **(b)** An original photograph of the Brunnen der Lebensfreude fountain in Rostock, Germany (courtesy of Bruce Miner). **(c)** and **(d)** Image samples, randomly selected from the set of all images that generated V1 model responses identical to the original (panel b). The value of the scaling parameter (used to determine the pooling regions of the model) was selected to yield 75% correct performance in discriminating such synthetic images (Fig. 4). While fixating the center (red circle) the two images should appear nearly identical to the original and to each other.

Nature Neuroscience: doi:10.1038/nn.2889

Supplementary analysis

We performed a meta-analysis to estimate the relationship between physiologically measured receptive field size and eccentricity in non-human primates. Measurements of receptive field sizes are variable across different experiments because different labs use different stimuli and mapping procedures [12, 13, 4]. To compare our psychophysics to physiology, we considered a wide range of data sets: four in V2 [8, 9, 3, 1], five in V1 [8, 10, 4, 7, 2], and three in V4 [9, 11, 5]. Two of these data sets are from owl monkey [1, 2], one from capuchin [10], and the rest are from macaque.

For each visual area, we combined data across experiments and estimated variability by pooling the raw data (rather than the fits), matching sample sizes, and resampling multiple times to obtain a 95% confidence interval on the slopes. Specifically, we determined the minimum number of cells across the data sets, and on each iteration of a bootstrap, resampled that number with replacement from each data set, and reestimated the slope of size versus eccentricity from the pooled data. We fit the data with a two-parameter hinged line, with a constant minimum size over some small range of eccentricities, followed by a linear relationship with some slope. For consistency, we used this "hinged line" model to estimate all slopes, but we obtained similar results when using a linear fit through 0. We also considered a straight line with variable intercept and slope [6], but the hinged line fits the data well (error was comparable for the two fits) and is better matched to the parameterization of our model. Variability across data sets tended to be largest at far eccentricities, and given that our visual stimuli only extended to 12.25 deg, we restricted our analysis of the physiology data to this range. In some of the cited studies [8, 10, 9, 7, 3, 5], rectangular receptive field sizes were mapped using a minimum response field procedure. To convert these numbers to diameters of circular receptive fields, and partially compensate for the bias toward smaller values inherent in this mapping technique [13, 4], we took the average of the diameter associated with the corners and sides of the squares (i.e., we multiplied the reported diameters by $(1 + \sqrt{2})/2$). Small modifications to any of these aspects of the data analysis did not qualitatively change the comparison between our psychophysics and the physiology (Figure 5).

References

[1] J M Allman and J H Kaas. Representation of the visual field in striate and adjoining cortex of the owl monkey (aotus trivirgatus). *Brain Res*, 35(1):89–106, Dec 1971.

[2] J M Allman and J H Kaas. The organization of the second visual area (v ii) in the owl monkey: a second order transformation of the visual hemifield. *Brain Res*, 76(2):247–65, Aug 1974.

[3] A Burkhalter and D C Van Essen. Processing of color, form and disparity information in visual areas vp and v2 of ventral extrastriate cortex in the macaque monkey. *J Neurosci*, 6(8):2327–51, Aug 1986.

[4] J R Cavanaugh, W Bair, and J A Movshon. Nature and interaction of signals from the receptive field center and surround in macaque v1 neurons. *Journal of Neurophysiology*, 88(5):2530–46, Nov 2002.

Nature Neuroscience: doi:10.1038/nn.2889

[5] R Desimone and S J Schein. Visual properties of neurons in area v4 of the macaque: sensitivity to stimulus form. *Journal of Neurophysiology*, 57(3):835–68, Mar 1987.

[6] S O Dumoulin and B A Wandell. Population receptive field estimates in human visual cortex. *Neuroimage*, 39(2):647–60, Jan 2008.

[7] D C Van Essen, W T Newsome, and J H Maunsell. The visual field representation in striate cortex of the macaque monkey: asymmetries, anisotropies, and individual variability. *Vision Res*, 24(5):429–48, Jan 1984.

[8] R Gattass, C G Gross, and J H Sandell. Visual topography of v2 in the macaque. *J Comp Neurol*, 201(4):519–39, Oct 1981.

[9] R Gattass, A P Sousa, and C G Gross. Visuotopic organization and extent of v3 and v4 of the macaque. *J Neurosci*, 8(6):1831–45, Jun 1988.

[10] R Gattass, A P Sousa, and M G Rosa. Visual topography of v1 in the cebus monkey. *J Comp Neurol*, 259(4):529–48, May 1987.

[11] W M Maguire and J S Baizer. Visuotopic organization of the prelunate gyrus in rhesus monkey. *J Neurosci*, 4(7):1690–704, Jul 1984.

[12] S Shushruth, J M Ichida, B Levitt, and A Angelucci. Comparison of spatial summation properties of neurons in macaque v1 and v2. *Journal of Neurophysiology*, 102(4):2069–2083, Oct 2009.

[13] G A Walker, I Ohzawa, and R D Freeman. Suppression outside the classical cortical receptive field. *Vis Neurosci*, 17(3):369–79, Jan 2000.